Top-down analysis of immunoglobulin G isotypes 1 and 2 with electron transfer dissociation on a high-field Orbitrap mass spectrometer.

Luca Fornelli[1¶], Daniel Ayoub[1Δ], Konstantin Aizikov[2], Xiaowen Liu[3,4], Eugen Damoc[2], Pavel A. Pevzner[5], Alexander Makarov[2], Alain Beck[6], and Yury O. Tsybin[1,7*]

[1] Biomolecular Mass Spectrometry Laboratory, Ecole Polytechnique Fédérale de Lausanne, 1015 Lausanne, Switzerland

[2] Thermo Fisher Scientific GmbH, 28199 Bremen, Germany

[3] Department of BioHealth Informatics, Indiana University-Purdue University Indianapolis, 46202 Indianapolis, IN, USA

[4] Center for Computational Biology and Bioinformatics, Indiana University School of Medicine, 46202 Indianapolis, IN, USA

[5] Department of Computer Science and Engineering, University of California in San Diego, 92093 San Diego, CA, USA

[6] Centre d'Immunologie Pierre Fabre, 74160 St Julien-en-Genevois, France

[7] Spectroswiss Sàrl, EPFL Innovation Park, 1015 Lausanne, Switzerland

---

This is the author's manuscript of the article published in final edited form as:
Fornelli, L., Ayoub, D., Aizikov, K., Liu, X., Damoc, E., Pevzner, P. A., … Tsybin, Y. O. (2017). Top-down analysis of immunoglobulin G isotypes 1 and 2 with electron transfer dissociation on a high-field Orbitrap mass spectrometer. Journal of Proteomics, 159, 67–76. https://doi.org/10.1016/j.jprot.2017.02.013

*Correspondence should be addressed to Dr. Yury O. Tsybin, Spectroswiss Sàrl, EPFL Innovation Park, Building I, 1015 Lausanne, Switzerland. Email: tsybin@spectroswiss.ch, phone +41 21 693 98 06

¶ Present address: Northwestern University, 2170 Campus Dr, 60208 Evanston, IL, USA

Δ Present address: Luxembourg Institute of Health, 1445 Strassen, Luxembourg

Running title: Top-down ETD of IgGs on Orbitrap Elite

List of abbreviation:

Automatic gain control, AGC

Electron transfer dissociation, ETD

Electron transfer dissociation – higher energy collisional dissociation, EThcD

Fourier transform mass spectrometry, FTMS

Keywords: electron transfer dissociation, ETD; immunoglobulin G, IgG; Orbitrap, top-down

Manuscript date: June 29, 2017

(Abstract)

The increasing importance of immunoglobulins G (IgGs) as biotherapeutics calls for improved structural characterization methods designed for these large (~150 kDa) macromolecules. Analysis workflows have to be rapid, robust, and require minimal sample preparation. In a previous work we showed the potential of Orbitrap Fourier transform mass spectrometry (FTMS) combined with electron transfer dissociation (ETD) for the top-down investigation of an intact IgG1, resulting in ~30% sequence coverage. Here, we describe a top-down analysis of two IgGs1 (adalimumab and trastuzumab) and one IgG2 (panitumumab) performed with ETD on a mass spectrometer equipped with a high-field Orbitrap mass analyzer. For the IgGs1, sequence coverage comparable to the previous results was achieved in a two-fold reduced number of summed transients, which corresponds, taken together with the significantly increased spectra acquisition rate, to ~six-fold improvement in analysis time. Furthermore, we studied the influence of ion-ion interaction times on ETD product ions for IgGs1, and the differences in fragmentation behavior between IgGs1 and IgG2, which present structural differences. Overall, these results reinforce the hypothesis that gas phase dissociation using both energy threshold-based and radical-driven ion activations is directed to specific regions of the polypeptide chains mostly by the location of disulfide bonds.

1. Introduction

Monoclonal antibodies (mAbs) are an effective therapeutic tool in a variety of medical conditions such as cancer and inflammatory disease.[1] These large glycoproteins constitute the fastest growing class of biotherapeutics.[2, 3] The main class of antibodies employed as biopharmaceuticals is immunoglobulin G (IgG). IgGs are large (~150 kDa) biomolecules with a quaternary structure made of two ~25 kDa light and two ~50 kDa heavy chains, identical among themselves, with the latter being N-glycosylated, Supporting Information Figure S1. The four chains are interconnected and their tertiary/quaternary structure is reinforced by inter- and intra-molecular disulfide bridges. Heavy chains can be translated from different genes, and their sequence determines the so-called IgG isotype (or subclass). In the pharmaceutical industry, three of the four IgG isotypes are of interest: IgG1, IgG2, and IgG4. Although all isotypes share ~90% of homology in their amino acid sequences, the structure of their hinge regions and the disulfide bond connectivity differ significantly. IgG1 and IgG4 contain 16 disulfide bridges, two in the hinge region linking the heavy chains, one disulfide bridge linking each light chain to the corresponding heavy chain and 12 intramolecular bridges (2 and 4 for each light and heavy chain, respectively). IgG2 contains 18 disulfide bonds with four in the hinge region linking the two heavy chains together.[4, 5] Figure S1 compares the structures of an IgG1 and an IgG2. Note that the C-terminal cysteine of the light chain is linked to the third cysteine (from the N-terminus) of the heavy chain in IgG2 (and also IgG4), whereas in IgG1 it is linked to the fifth cysteine.

Due to their relevance as biotherapeutics, and with the raise of the so-called biosimilars in the pharmaceutical market,[3, 6] high-throughput and extensive characterization of the sequence and structure of IgGs is needed.[2] Mass spectrometry (MS) plays a pivotal role in analysis of IgGs. MS-based methods have been developed and implemented across all stages of mAb production.[4] The basic workflow may include intact IgG mass measurement, IgG fragment (reduced light and heavy chains or papain-produced fragments) mass measurement (referred to as middle-up MS approach),[7] middle-down,[8, 9] extended bottom-up[10] and bottom-up MS[2, 11] approaches. Although bottom-up approaches provide the most structural information today, they suffer a number of drawbacks such as artifact introduction and lengthy sample preparation.[12-14] Top-down mass spectrometry (TD MS)[15] refers to the gas-phase dissociation of intact biomolecules and subsequent mass measurement of the fragmentation products. Applied to IgGs, TD MS is a convenient way to obtain primary structure information without the need of reducing the inter-chain disulfide bonds in solution. Furthermore, this approach generally allows access to sequence confirmation of terminal regions as well as variable domains. It also allows the identification and localization of major modifications and the characterization of major glycoforms.[16] It has the advantage of requiring a highly simplified sample preparation and therefore minimal artifact introduction induced by sample processing. Despite these advantages, TD MS is not yet routinely used for the characterization of mAbs, primarily due to the large number of highly charged products yielded by IgG fragmentation, which requires

high-resolution MS and the applications of techniques aimed at improving sensitivity, such as spectral summation (averaging).[17]

Electron capture dissociation (ECD)[18, 19] and electron transfer dissociation (ETD)[20] of whole proteins usually generate larger sequence coverage than slow-heating activation methods (such as collision-induced dissociation, CID).[21] ECD and ETD MS/MS are also known as powerful methods for characterization of labile post-translational modifications, e.g., glycosylation.[22, 23] Fourier transform ion cyclotron resonance (FT-ICR) MS provides the highest resolution and can be hyphenated with ECD, making it the technique of choice for earlier TD MS experiments.[24-26] Notably, Mao *et al.* achieved 25% sequence coverage of a purified IgG1 using qFT-ICR MS and ECD when isolating a single charge state in a direct infusion ionization mode. They increased the sequence coverage to ~33% with a broadband tandem mass spectrometry (MS/MS), e.g., using all the IgG1 ions present in the charge state envelope as precursors for ECD.[27] However, the general use of FT-ICR MS instruments for IgG characterization is rare,[4] presumably due to their limited presence in biopharmaceutical laboratories owing to the tedious maintenance and operational costs, as well as oftentimes low efficiency of heavy precursor ion transfer and capture in the ICR cells for subsequent ECD reaction.

With the advent of ETD efficiently performed in an external ion trap with product ion detection in a high-resolution mass analyzer, e.g., Orbitrap FTMS[28], FT-ICR MS,[29] or time-of-flight (TOF) MS,[30, 31] the performance of TD MS has improved. Particularly, TD MS of proteins on-line separated with

reversed phase liquid chromatography (LC) prior to electrospray ionization (ESI) became possible routinely.[32, 33] We have previously described the use of ETD with a high-resolution qTOF MS reporting the overall sequence coverage of 21% for mouse IgG1 and 15% for human IgG1 which provided structural information on variable domains of both the heavy and the light chain.[34] As a result of a more extensive investigation, we achieved 33% sequence coverage of a human IgG1 using ETD with a hybrid linear ion trap-Orbitrap FTMS (considering *c*-, *z*- and *y*-type product ions) equipped with a standard (moderate electric field, D30 type) Orbitrap mass analyzer (Orbitrap Velos Pro). The results obtained with narrow (i.e., 100 *m/z*) and large (i.e., 600 *m/z*) isolation windows for precursor ions were combined to increase the final number of identified product ions.[17] In all the aforementioned TD MS studies, over one thousand (micro)scans (or transients in a time-domain domain, in the case of FTMS) were summed (averaged) to boost the sequence coverage.[17, 27, 34] Typically, several LC MS/MS runs were acquired followed by data summation (averaging) to provide the increased number of scans. The current state-of-the-art in TD MS, however, does not enable the full sequencing of the disulfide bond protected domains of light or heavy chain, neither it allows the direct localization of the glycosylation site in the C_H2 domain of the heavy chain. This is due to the compact protein structure and its disulfide bond network (see Supporting Information, Figure S1), which is believed to constitute the major limitation in IgG TD MS characterization. Overall, the performance of all three approaches, using ETD on

a qTOF MS or on a linear trap-Orbitrap FTMS, as well as ECD on FT-ICR MS, provide comparable results.

Here we investigated the potential of ETD implemented on a high-field compact Orbitrap FTMS, namely the Orbitrap Elite,[35] for faster top-down characterization of three therapeutic mAbs: adalimumab and trastuzumab (both of the IgG1 subclass), and the IgG2 panitumumab. The high-field Orbitrap mass analyzer is characterized by a higher frequency of ion oscillations along the central electrode compared to the prior generation of Orbitrap mass analyzers.[36, 37] Increased frequency of ion oscillations leads to the corresponding enhancement of the resolving power over a fixed acquisition time. Moreover, the implementation of a mixed absorption and magnitude mode FT of spectral representation (known as enhanced FT, or eFT algorithm)[38] allows a further gain (of up to two-fold) in acquisition rate at a constant resolution.[39] In addition to the advantages of the employed mass analyzer, we optimized precursor ion isolation and product ion transfer between the linear trap and the Orbitrap to increase the efficiency of ETD-based TD MS. Finally, IgG TD MS was performed under the optimized conditions with a two-stage ion activation method, a combination of ETD and higher-energy collision dissociation (HCD)[40] termed EThcD,[41] which has been recently applied to TD MS experiments, demonstrating sequence complementarity with ETD.[42, 43]

2. Materials and methods

2.1 Chemicals. Water, acetonitrile (ACN), methanol (MeOH), formic acid (FA) and trifluoroethanol (TFE) were obtained in LC-MS purity grade. Water, ACN and MeOH were purchased from Fluka Analytical (Buchs, Switzerland). FA was obtained from Merck (Zug, Switzerland), and TFE from Acros Organics (Geel, Belgium).

2.2 Sample preparation. Therapeutic monoclonal antibodies of the IgG1 class, namely adalimumab (Humira, Abbott Laboratories) and trastuzumab (Herceptin, Genentech), as well as the IgG2 panitumumab (Vectibix, Amgen) are the European Medicines Agency approved versions and formulations, available commercially to the general public. Prior to direct infusion analysis, all antibodies were buffer exchanged against a 150 mM ammonium acetate solution pH 6.7 using Micro-Spin desalting columns (Zeba 75 µL, Thermo Fisher Scientific, Zug, Switzerland).

2.3 Sample delivery and ionization. The antibodies were injected into the mass spectrometer either by on-line coupled LC or by direct infusion in a positive ion mode of ESI. In the former case, we employed an UltiMate 3000 LC system (Thermo Fisher Scientific) equipped with a reversed phase C4 column (Hypersil Gold, 1x100 mm, 5 µm particle size, Thermo Fisher Scientific, Runcorn, UK), applying a gradient of ACN from 5 to 80% in 20 min, in presence of 0.1% FA, and

a flow rate of 100 µl/min generated by the loading pump. 1.5 µg of antibody (~10 pmol), diluted in 20% ACN and 0.1% FA, were typically loaded in each injection, resulting in ~2 min elution of the IgG. The IonMax ion source (Thermo Fisher Scientific) was operated at 3.7 kV, with sheath gas set to 20 and auxiliary gas to 10 arbitrary units. In the latter case, the antibody, buffer exchanged as described above, was diluted in 50% ACN and 0.1% FA to a final concentration of ~10 µM; 6 µl of this IgG solution were loaded in a 20 µl loop connected to the injection valve of the LC system and infused through a silica capillary to the nanoESI source (Nanospray Flex ion source, Thermo Fisher Scientific) equipped with a metallic emitter to which a 2.4 kV voltage was applied. The composition of the solution used to push the IgG from the loop to the source was 39.9% water, 30% ACN, 20% MeOH, 10% TFE, and 0.1% FA. The flow rate generated by the nano-pump of the LC system was 0.6 µl/min.

2.4 Mass spectrometry. All experiments were performed on a hybrid dual linear ion trap high-field Orbitrap FT mass spectrometer (Orbitrap Elite, Thermo Scientific, Bremen, Germany) equipped with ETD and HCD. Similarly to our previous report,[17] the S-lens RF level was set to 70% and the temperature of heated transfer capillary was 350° C. Broadband mass spectra of intact IgGs and tandem mass spectra of the same molecules were recorded in separate experiments using ion detection in the Orbitrap FTMS (*m/z* 200-4000). All Orbitrap FTMS scans were recorded averaging 10 microscans to improve the SNR. Orbitrap FTMS was calibrated in the high mass range (*m/z* 2000-4000)

using ion at 2021.93954 *m/z* of commercial LTQ Velos ESI Positive Ion Calibration Solution (Thermo Fisher Scientific). Intact mass measurements of IgGs were performed at 15'000 resolution at 400 *m/z* with a target value of charges (automatic gain control, AGC) of 1 million. For ETD experiments, precursor ions were isolated between *m/z* 2400 and 2900 in the high pressure LTQ and subsequently subjected to ETD reaction. The AGC value for fluoranthene radical anions was set to 2 million charges, anion maximum injection time was set to 50 ms and ETD duration (i.e., ion-ion interaction time) was set either to 10 or 25 ms. Product ion detection in the Orbitrap mass analyzer was performed with 120'000 resolution (at 400 *m/z*, eFT enabled) and an AGC for precursor ions of 1 million charges.

For both intact mass measurements and MS/MS, the gas (N_2) "delta pressure" was of 0.1E-10 torr. The delta pressure corresponds to the difference in the pressure measured in the so-called ultra-high vacuum region (i.e., UHV region, or Orbitrap chamber) when nitrogen is injected into the HCD cell and when the gas is completely shut down. A delta value of 0.1E-10 torr likely corresponds to a pressure of ~1-2 mtorr of N_2 in the HCD cell. Typically the delta pressure for bottom-up proteomics (i.e., smaller size ions) is ~0.35E-10 torr. Therefore, for TD MS the N_2 gas pressure in the HCD cell is reduced compared to the bottom-up proteomics. To further improve ion transmission to the high-resolution mass analyzer from the linear trap, ions ejected from the linear trap were first collisionally cooled in the HCD cell (a technique known as "HCD

trapping"), then transferred backward to the C-trap, and finally injected into the Orbitrap as previously described.[44]

EThcD experiments were performed as follows. After ETD with 10 ms duration, all ETD products, including both charge-reduced species and product ions (precursors are generally completely consumed in ETD under the applied conditions), were transferred from the linear trap to the HCD cell. Here an axial potential was set to 25 or 40 V, so that instead of ion capture and relaxation a second ion activation event could occur. Finally, ions were transferred back to the C-trap and further into the Orbitrap for detection.

2.5 FTMS data processing and analysis. The data processing routine for obtaining tandem mass spectra with an improved SNR was performed as previously described.[17] Briefly, in both LC-MS/MS and direct infusion MS/MS experiments, Orbitrap FTMS time-domain transients were recorded in MIDAS .dat format[45] and underwent summation (averaging) before being processed for time-to-frequency conversion. In this way it was possible to sum 384 ms transients derived from separate LC runs or distinct direct infusion experiments. Enhanced Fourier transform, eFT, or a standard magnitude mode Fourier transform, mFT, was then applied to process transients and yield frequency-domain spectra (internal processing at Thermo Fisher Scientific).[38] The thus obtained frequency spectra were then converted into .RAW mass spectra (internal processing at Thermo Fisher Scientific) for further viewing and processing with XCalibur software (Thermo Fisher Scientific), as well as data analysis (*vide infra*).

Final ETD mass spectra were derived from summed transients recorded for 10 and 25 ms ETD duration experiments. For an in-depth evaluation of the effect of ETD duration on IgG fragmentation, 10 and 25 ms ETD datasets were also analyzed separately. The resolution gain of eFT versus mFT is known to be two-fold.[38] However, to demonstrate the practically useful and presumably sufficient resolution requirement for analysis of top-down ETD mass spectra of IgGs, only the mFT-processed data are reported here. Results obtained with eFT signal processing were found to be comparable to the mFT processing in terms of protein sequence coverage (data not shown).

Previously, the combination of Xtract deconvolution software and ProSight PC 3.0 product ion assignment software (both from Thermo Fisher Scientific) was successfully employed for IgG TD MS data analysis.[30] Here, we extended this approach by adding a workflow combining the MS-Deconv deconvolution algorithm and MS-Align+ product ion assignment software (both developed at University of California San Diego, CA, USA).[46] A comparison between the results produced by MS-Deconv/MS-Align+ and by Xtract/ProSight PC is presented in Figure S2, Supporting Information. Both the data analysis packages led to comparable results. In greater detail, the MS-Deconv/MS-Align+ analyses were realized according to the following steps: (i) ReAdW software was used to convert .RAW files of ETD mass spectra into centroided mzXML files; (ii) a customized version of MS Deconv was used to deconvolute the mzXML files using a SNR cutoff of 3. The custom version of MS-Deconv was written to process the data sets containing MS/MS information only, whereas the standard version of

MS-Deconv requires both MS and the directly corresponding to it MS/MS data sets; (iii) MS-Align+ was used for product ion identification, considering *c*- and *z*·- type ions for ETD experiments and *c*-, *z*·-, *b*- and *y*-type ions for EThcD data. Cysteine residues were considered as not modified and all the mass tolerances were set to 20 ppm. Manual validation was performed for cleavage sites identified from product ions present only in a single charge state. The graphical fragmentation maps reported herein were realized using either ProSightPC or ProSight Lite software.[47]

2.6 Product ion abundance analysis. Abundances of identified product ions were derived from MS-Align+ analysis. For each cleavage site, all the related product ions were considered and grouped. Final abundances were obtained by dividing the abundance values reported for each product ion over the ion charge state, and summing all the resulting charge-normalized abundance values of product ions generated from a single cleavage site. For plotting together product ion abundance (PIA) analysis results of different sets of data, the abundances were expressed as relative percentages of the most abundant product ion cluster (i.e., the group of all the *z*-type ions, with different charge state, derived from a single cleavage site) in each data set.

3. Results and discussion

3.1 Optimization of ETD MS/MS of IgG. To maximize ETD efficiency, we sought to first optimize precursor cation selection and product ion transfer. In the

former work based on an Orbitrap Velos Pro mass spectrometer we isolated adalimumab precursor ions around *m/z* 2750 (isolation window width: 100 *m/z*, precursor ions from 53+ to 55+) or 2900 (isolation window width: 600 *m/z*, precursor ions from 47+ to 57+). Considering the charge state envelope obtained with the current LC-MS setting on the Orbitrap Elite for intact adalimumab, we centered the isolation window at *m/z* 2700, with a width of 600 *m/z*, thus including precursors from 50+ to 61+ (Figure S3, Supporting Information). Higher charge state precursor ions are supposed to increase the fragmentation efficiency in ETD and facilitate the separation of obtained product ions bound by non-covalent bonds. Furthermore, cleavage preferences within protein structure shift as a function of charge location. In regard to product ion transfer, we applied a combination of reduction of the gas pressure in the HCD cell and the "HCD trapping" technique, *vide supra*. The gas pressure reduction improves SNR of large product ions by improving their transmission from LTQ into the HCD cell and further within the Orbitrap analyzer. Trapping of ions in the HCD cell (and not directly and only in the C-trap) allows the improved transmission also of lighter ions, presumably counterbalancing the reduced damping effect in the C-trap resulting from the lower gas pressure (Figure S4, Supporting Information).

Overall, the implementation of these settings allowed for SNR increases in the MS/MS mode for high *m/z* ions, which resulted in a reduction of the number of transients that needed to be summed to obtain high-quality mass spectra in comparison to our previous work, *vide infra*. Each ETD mass spectrum derived

from a combination of transients was obtained applying two different ion-ion interaction times, 10 and 25 ms, **Figure 1**. These two ETD durations were chosen to allow a direct comparison with our previous work, where we combined ETD MS/MS data resulting from shorter and longer ion-ion interaction times, pre-selected for fragmentation of intact denatured IgG precursor ions. Increasing ETD duration enhanced the formation of product ions with a reduced charge state, likely because of the occurrence of multiple electron transfer and consequent charge reduction events. Nevertheless, the separate analysis of mass spectra obtained with 10 or 25 ms ETD duration revealed that most of the identified cleavage sites are shared between the two experiments (see product ion abundance analysis results below), suggesting that ETD is primarily limited by the retention of a compact conformation of the IgG in the gas phase. Summing transients from these two experimental sets, though, increased the confidence in the assignment of cleavage sites, as product ions obtained by the same backbone cleavage are identified in multiple charge states.

3.2 ETD and EThcD MS/MS of intact human IgG1. The analysis of product ions obtained by ETD MS/MS was performed for two IgG1 mAbs, adalimumab and trastuzumab. Their sequences are 92% homologous, the differences being almost entirely localized to the complementarity determining regions (CDRs) involved in the antigen binding. **Figure 2 A** displays the ETD fragmentation map of adalimumab, with the typical fragmentation pattern expected for this IgG isotype. Extensive fragmentation is achieved on the heavy chain for the loop

interconnecting V_H and C_H1, the loop between C_H2 and C_H3 and part of the C_H3 domain; on the light chain, the characterized region is represented by the loop between V_L and C_L. For both chains, therefore, the sequenced areas are mainly disulfide bond-free loops exposed to the solvent. The results of ETD MS/MS application to trastuzumab are nearly identical to those for adalimumab (Figure S5, Supporting Information). For both the IgGs only the CDR3 domains of light and heavy chains are fully sequenced, and only a few product ions positioned on CDR2 of heavy and light chain have been assigned for trastuzumab (which shows slightly higher sequence coverage). As summarized in **Table 1**, 310 ETD MS/MS scans (which corresponds to 3100 microscans or transients) were summed to result in 23.8% and 26.5% sequence coverage for adalimumab and trastuzumab, respectively. Notably, from the comparison of these results and the previously reported ones it is apparent how, although the total sequence coverage (i.e., sum of cleavages in light and heavy chains) is similar, the distribution of identified cleavage sites between the two chains is changed, with the heavy chain being more sequenced in the present report than in the previous one. For trastuzumab we reached 29% sequence coverage which represents the highest value obtained so far for the heavy chain of an intact IgG1 by ETD TD MS. On the other hand, the light chain has been less sequenced with the new settings and data analysis routine than in the past, but also for the drastically reduced number of scans considered. Manual inspection of MS/MS spectra reveals that the missing product ions are mainly those arising from cleavage sites located at the two termini of the light chain: these are light, lowly charged ions that presumably

were not favorably transmitted with the newly employed settings (Figure S4, Supporting Information). The fully sequenced region in the light chain, corresponding to the loop between V_L and C_L, as mentioned above, remained the same between the two studies, and it is equal between adalimumab and trastuzumab (both of which often show complementary *c*- and *z*-type ions for the same cleavage site). Cleavages outside this area do not follow any clear pattern and seem randomly distributed.

To improve the sequence coverage of the IgG1 and, specifically, of the light chain, we applied EThcD on adalimumab. We summed transients obtained with EThcD (i.e., both product ions and charge-reduced species) performed at both 25 and 40 V. As shown in Figure 2B, EThcD produced fragmentation mainly in the same areas previously covered by ETD, but also induced new cleavages at the N-terminus of both light and heavy chain, and provided *b*- and *y*-type ions from the N-terminal side of proline that could not be previously identified from ETD data. The sequence coverage for the heavy chain of adalimumab is lower than for ETD, but it passed from ~19% to ~28% for the light chain, as reported in Table 1. Overall, the combination of 310 ETD scans and 260 EThcD scans, for a total of 570 scans, produced 30.5% sequence coverage, which is the same result obtained by averaging 1360 scans in our previous work based on the Orbitrap Velos Pro. In addition to the reduced number of scans, a two-fold scan speed improvement due to the implementation of the high-field Orbitrap mass analyzer (higher frequency of ion axial oscillations) decreased the required experimental time for mFT signal processing. Further two-fold improvement can

be achieved by the application of eFT signal processing. For instance, at 120'000 resolution (at 400 *m/z*, eFT signal processing) and under LC-MS/MS conditions, 120 transients (microscans) could be recorded per minute of IgG elution on the Orbitrap Elite FTMS versus the previous 40 transients (microscans) on the Orbitrap Velos Pro (mFT signal processing, 100'000 resolution at 400 *m/z*). The ETD MS/MS experimental sequence, including cation accumulation, anion injection and subsequent cation/anion interaction largely contributes to the duty cycle, partially counterbalancing the time gain in FTMS data acquisition due to combination of high-field Orbitrap and eFT.

Finally, from the comparison of the ETD TD MS results obtained with different ion transfer parameters (especially the pressure conditions in the HCD cell), those reported here and in the previous work, it seems beneficial to acquire ETD TD MS data with both conditions and pool the data together. Indeed, results reported in Figure S6 (Supporting Information) show that the sequence coverage for ETD MS/MS of adalimumab with only *c* and *z*-ions is increased to 41.3% and 34.7% for light and heavy chain, respectively, with a total sequence coverage of 36.8%.

3.3 Product ion abundance analysis of ETD MS/MS of IgGs1. A PIA analysis was conducted on ETD MS/MS data for the C-terminal portions of the almost completely sequenced heavy chains of the investigated IgGs1. **Figure 3** shows a comparison between the relative abundances of *z*-ions from 10 ms ETD of adalimumab, as well as 10 ms and 25 ms ETD of trastuzumab. Note that the

two IgGs share identical sequence in the analyzed area. For all three data sets, the average abundance of product ions generated by the disulfide-free loop connecting C_H2 and C_H3 is ~40% of the maximum, and global maxima are all located there. Conversely, ions derived from the disulfide-protected area of C_H3, as well as those from the disulfide-free C-terminal end (which is, structurally speaking, a part of the C_H3 domain), generally have an abundance lower than 10% of the corresponding maximum. Furthermore, the global maxima for the two 10 ms ETD data sets are both located at the cleavage site between K_{105} and G_{106} (which results in z_{106} ions). Other local maxima correspond to the formation of z_{96}, z_{93}, and z_{86} ions. The 25 ms data set shows a similar trend, with z_{106} still abundant but surpassed by z_{93}, z_{91}, and z_{86}. Therefore, the ETD results are conditioned by the secondary and tertiary structures of the gaseous protein ions. Moreover, similarly to ECD MS/MS,[48] the ETD radical process seems to be affected by the electron transfer site, as the presence of basic residues at one side of the cleavage maxima would suggest. Finally, the shift in maxima occurring when passing from 10 to 25 ms ETD might be explained by the increased probability of secondary electron transfer events when the ETD duration is prolonged. The occurrence of secondary electron transfer and consequent charge neutralization events might be confirmed by the reduced average charge state of the product ions identified for 25 ms ETD in comparison to 10 ms ETD experiments (Table S1, Supporting Information). The data suggest that these events are most prominent at the flexible loop and with a C_H3 domain in a compact conformation. Therefore, despite the second fragmentation event,

the abundance of product ions originated within the sequence of the C_H3 domain is not higher than for the 10 ms experiments. Instead, we observe the shift between z_{106} and z_{86} as maxima in the disulfide-free region. Visually, this is represented in **Figure 4** through a color-coded map based on crystal structure of trastuzumab (image elaborated with The PyMol Molecular Graphics System, version 1.3, Schrodinger, LLC). The passage from 10 ms to 25 ms ETD duration induces the translation of highly frequent cleavage sites (represented in red) towards the C-terminus, but still in solvent accessible positions. On the contrary, the compact "immunoglobulin-like domain" corresponding to C_H3, which resembles the structure of a beta barrel, and contains an intra-molecular disulfide bridge, remains poorly sequenced (and thus represented in black-blue). These results reinforce the hypothesis that IgGs retain a relatively compact high-order structure in the gas phase, even under denaturing ionization conditions.

3.4 ETD MS/MS of intact human IgG2. ETD MS/MS was performed on panitumumab, an IgG2, to provide a confirmation to our hypothesis that limitations in sequence coverage achieved for IgGs1 are mainly attributable to gas-phase retention of a structured, compact conformation by the protein. As displayed in **Figure 5**, identified product ions for this IgG are localized in the areas sequenced in the experiments involving adalimumab and trastuzumab, e.g., the solvent accessible loops interconnecting consecutive disulfide-protected domains and the C_H3 domain. In-depth analysis reveals that the C-terminal portion of the heavy chain is highly sequenced, with 83 assigned *z*-type ions

versus 82 *z*-ions identified for trastuzumab, which has overall the highest sequence coverage for its heavy chain (Table 1). Nevertheless, given that, in accordance to what is observed for IgGs1, the hinge region is not sequenced also in the case of panitumumab, differences between the two IgG isotypes are present in the loop interconnecting V_H and C_H1. In the case of IgGs1, this loop was fully sequenced, whereas for panitumumab only partial sequencing was achieved. This can be explained by the presence in the loop of the IgG2 of Cys_{133}, involved in an inter-molecular disulfide bridge connecting the heavy with the light chain. Notably, most of the identified *c*-type product ions are located to the N-terminus of C_{133}. Further studies are needed to determine whether ETD cleavages were primarily impeded in the portion of the loop at the C-terminal side of C_{133} or, conversely, cleavages occurred but primarily produced product ions with portions of the light chain still present and were therefore not identifiable by the present version of the data analysis approach. Finally, panitumumab's light chain has been sequenced in its central area (i.e., disulfide-free loop between V_L and C_L), similarly to IgGs1, but its incomplete sequencing and, importantly, the limited number of identified *z*-ions (nine, corresponding to only ~50-30% of those assigned in the other experiments), could indicate that the inter-molecular disulfide bridge with the heavy chain is less efficiently cleaved in IgG2 than in IgG1.

4. Concluding remarks

Developments in Orbitrap FTMS technology mark a substantial improvement in top-down MS performance. Experimentally, around three-fold faster acquisition of IgG ETD data under optimized conditions in the Orbitrap Elite (high-field compact Orbitrap analyzer) combined with a more than two-fold reduction in the number of transients to be summed as required for a comprehensive top-down analysis of IgGs resulted in about six-fold reduction of acquisition time in the present study relative to the analysis with the Orbitrap Velos Pro. For the latter, a standard trap with mFT yielded resolution of 100'000 at 400 *m/z*. Here, resolution of 60'000 (at 400 *m/z*) was provided with mFT signal processing and 120'000 (at 400 *m/z*) when eFT algorithm was employed. The (moderate) level of product ion spectral complexity generated in this top-down experiment, perhaps due to a symmetric subunit structure of IgGs, demonstrated similar performance in sequence coverage for mFT and eFT-generated mass spectra. The following factors contributed to the reduction of number of scans needed for high quality TD MS analysis: (i) selection of higher charged precursors, (ii) optimization of transfer of large ETD product ions from the linear trap to the Orbitrap by lowering the HCD cell gas pressure, (iii) combination of experiments conducted with different ion-ion reaction times, and (iv) use of EThcD with two different collisional energy values. Nevertheless, the previously determined limit in sequence coverage, ~30%, could not be overcome. The primary cause for the limited sequence coverage is the gas-phase retention of highly structured areas in the IgG, mainly in correspondence of the immunoglobulin-like domains.

To facilitate user access to the described technology, algorithms and methods for spectral summation across different experiments or/and for transient acquisition and subsequent signal processing (absorption mode FT) of summed transients where needed by spectral complexity have been made commercially available (Spectroswiss, Lausanne, Switzerland). Further extending the sequence coverage in TD MS of IgGs may be provided by an improved ETD reaction cell,[49] chemical ionization source for front-end ETD on Orbitrap FTMS,[50] and the use of ion activation methods alternative to ETD, e.g., ultraviolet photodissociation.[51] Furthermore, improved sequence coverage is achievable by combining ETD experimental data acquired with high HCD gas pressure (i.e., maximizing light product ion transmission), and low gas pressure (i.e., maximizing heavy product ion transmission), as it results from the combination of present data with those acquired in standard operational conditions with the Orbitrap Velos Pro. Finally, the probable presence of internal products and product ions retaining parts of both light and heavy chains bonded by inter-molecular disulfide bridges will require developments in the data analysis tailoring this specific class of proteins.

5. Acknowledgements

We thank Kristina Srzentić and Anton Kozhinov for discussions and technical support. We express our gratitude to Thermo Fisher Scientific for providing access under license to Orbitrap Elite FTMS transient signals and related functionality enabled by the developers' kit. The work was supported by the

Swiss National Science Foundation (Projects 200021-125147 and 200021-147006) and the European Research Council (ERC Starting grant 280271 to YOT). Xiaowen Liu was supported by the National Institute of General Medical Sciences, National Institutes of Health (NIH) through Grant R01GM118470.

6. References

[1] A. Beck, S. Sanglier-Cianferani, A. Van Dorsselaer, Biosimilar, biobetter, and next generation antibody characterization by mass spectrometry, Anal Chem 84(11) (2012) 4637-46.

[2] D. Ayoub, W. Jabs, A. Resemann, W. Evers, C. Evans, L. Main, C. Baessmann, E. Wagner, D. Suckau, A. Beck, Correct primary structure assessment and extensive glyco-profiling of cetuximab by a combination of intact, middle-up, middle-down and bottom-up ESI and MALDI mass spectrometry techniques, MAbs 5(5) (2013) 0--1.

[3] G. Walsh, Biopharmaceutical benchmarks 2014, Nat Biotechnol 32(10) (2014) 992-1000.

[4] A. Beck, E. Wagner-Rousset, D. Ayoub, A. Van Dorsselaer, S. Sanglier-Cianferani, Characterization of therapeutic antibodies and related products, Anal Chem 85(2) (2013) 715-36.

[5] G. Vidarsson, G. Dekkers, T. Rispens, IgG subclasses and allotypes: from structure to effector functions, Front Immunol 5 (2014) 520.

[6] S.A. Berkowitz, J.R. Engen, J.R. Mazzeo, G.B. Jones, Analytical tools for characterizing biopharmaceuticals and the implications for biosimilars, Nat Rev Drug Discov 11(7) (2012) 527-40.

[7] B. Wang, A.C. Gucinski, D.A. Keire, L.F. Buhse, M.T. Boyne, Structural comparison of two anti-CD20 monoclonal antibody drug products using middle-down mass spectrometry, Analyst 138(10) (2013) 3058-3065.

[8] L. Fornelli, D. Ayoub, K. Aizikov, A. Beck, Y.O. Tsybin, Middle-down analysis of monoclonal antibodies with electron transfer dissociation orbitrap fourier transform mass spectrometry, Anal Chem 86(6) (2014) 3005-12.

[9] V.C. Cotham, J.S. Brodbelt, Characterization of Therapeutic Monoclonal Antibodies at the Subunit-Level using Middle-Down 193 nm Ultraviolet Photodissociation, Analytical chemistry 88(7) (2016) 4004-4013.

[10] K. Srzentic, L. Fornelli, U.A. Laskay, M. Monod, A. Beck, D. Ayoub, Y.O. Tsybin, Advantages of Extended Bottom-Up Proteomics Using Sap9 for Analysis of Monoclonal Antibodies, Analytical chemistry 86(19) (2014) 9945-9953.

[11] Z. Zhang, H. Pan, X. Chen, Mass spectrometry for structural characterization of therapeutic antibodies, Mass Spectrom Rev 28(1) (2009) 147-76.

[12] O.V. Krokhin, M. Antonovici, W. Ens, J.A. Wilkins, K.G. Standing, Deamidation of -Asn-Gly- sequences during sample preparation for proteomics: Consequences for MALDI and HPLC-MALDI analysis, Anal Chem 78(18) (2006) 6645-50.

[13] L.W. Dick, C. Kim, D.F. Qiu, K.C. Cheng, Determination of the origin of the N-terminal pyro-glutamate variation in monoclonal antibodies using model peptides, Biotechnology and Bioengineering 97(3) (2007) 544-553.

[14] K. Diepold, K. Bomans, M. Wiedmann, B. Zimmermann, A. Petzold, T. Schlothauer, R. Mueller, B. Moritz, J.O. Stracke, M. Molhoj, D. Reusch, P. Bulau, Simultaneous assessment of Asp isomerization and Asn deamidation in recombinant antibodies by LC-MS following incubation at elevated temperatures, PLoS One 7(1) (2012) e30295.

[15] T.K. Toby, L. Fornelli, N.L. Kelleher, Progress in Top-Down Proteomics and the Analysis of Proteoforms, Annu Rev Anal Chem (Palo Alto Calif) 9(1) (2016) 499-519.

[16] B.Q. Tran, C. Barton, J. Feng, A. Sandjong, S.H. Yoon, S. Awasthi, T. Liang, M.M. Khan, D.P. Kilgour, D.R. Goodlett, Y.A. Goo, Comprehensive glycosylation profiling of IgG and IgG-fusion proteins by top-down MS with multiple fragmentation techniques, J Proteomics 134 (2016) 93-101.

[17] L. Fornelli, E. Damoc, P.M. Thomas, N.L. Kelleher, K. Aizikov, E. Denisov, A. Makarov, Y.O. Tsybin, Analysis of intact monoclonal antibody IgG1 by electron transfer dissociation Orbitrap FTMS, Mol Cell Proteomics 11(12) (2012) 1758-67.

[18] R.A. Zubarev, N.L. Kelleher, F.W. McLafferty, Electron capture dissociation of multiply charged protein cations. A nonergodic process, Journal of the American Chemical Society 120(13) (1998) 3265-3266.

[19] R.A. Zubarev, D.M. Horn, E.K. Fridriksson, N.L. Kelleher, N.A. Kruger, M.A. Lewis, B.K. Carpenter, F.W. McLafferty, Electron capture dissociation for structural characterization of multiply charged protein cations, Analytical chemistry 72(3) (2000) 563-573.

[20] J.E.P. Syka, J.J. Coon, M.J. Schroeder, J. Shabanowitz, D.F. Hunt, Peptide and protein sequence analysis by electron transfer dissociation mass spectrometry, Proceedings of the National Academy of Sciences of the United States of America 101(26) (2004) 9528-9533.

[21] J.M. Wells, S.A. McLuckey, Collision-induced dissociation (CID) of peptides and proteins, Methods Enzymol 402 (2005) 148-85.

[22] S. Meier, Y. Tsybin, P. Dyson, B. Keppler, C. Hartinger, Fragmentation methods on the balance: unambiguous top–down mass spectrometric characterization of oxaliplatin–ubiquitin binding sites, Analytical and Bioanalytical Chemistry 402(8) (2012) 2655-2662.

[23] H. Molina, R. Matthiesen, K. Kandasamy, A. Pandey, Comprehensive Comparison of Collision Induced Dissociation and Electron Transfer Dissociation, Analytical chemistry 80(13) (2008) 4825-4835.

[24] Y. Ge, I.N. Rybakova, Q. Xu, R.L. Moss, Top-down high-resolution mass spectrometry of cardiac myosin binding protein C revealed that truncation alters protein phosphorylation state, Proc Natl Acad Sci U S A 106(31) (2009) 12658-63.

[25] S.G. Valeja, N.K. Kaiser, F. Xian, C.L. Hendrickson, J.C. Rouse, A.G. Marshall, Unit mass baseline resolution for an intact 148 kDa therapeutic monoclonal antibody by Fourier transform ion cyclotron resonance mass spectrometry, Anal Chem 83(22) (2011) 8391-5.

[26] J.D. Tipton, J.C. Tran, A.D. Catherman, D.R. Ahlf, K.R. Durbin, J.E. Lee, J.F. Kellie, N.L. Kelleher, C.L. Hendrickson, A.G. Marshall, Nano-LC FTICR tandem mass spectrometry for top-down proteomics: routine baseline unit mass resolution of whole cell lysate proteins up to 72 kDa, Anal Chem 84(5) (2012) 2111-7.

[27] Y. Mao, S.G. Valeja, J.C. Rouse, C.L. Hendrickson, A.G. Marshall, Top-down structural analysis of an intact monoclonal antibody by electron capture

dissociation-Fourier transform ion cyclotron resonance-mass spectrometry, Anal Chem 85(9) (2013) 4239-46.

[28] G.C. McAlister, W.T. Berggren, J. Griep-Raming, S. Horning, A. Makarov, D. Phanstiel, G. Stafford, D.L. Swaney, J.E. Syka, V. Zabrouskov, J.J. Coon, A proteomics grade electron transfer dissociation-enabled hybrid linear ion trap-orbitrap mass spectrometer, J Proteome Res 7(8) (2008) 3127-36.

[29] S. Bourgoin-Voillard, N. Leymarie, C.E. Costello, Top-down tandem mass spectrometry on RNase A and B using a Qh/FT-ICR hybrid mass spectrometer, Proteomics 14(10) (2014) 1174-1184.

[30] R.G. Hartmer, D.A. Kaplan, C. Stoermer, M. Lubeck, M.A. Park, Data-dependent electron transfer dissociation of large peptides and medium size proteins in a QTOF instrument on a liquid chromatography timescale, Rapid Commun Mass Spectrom 23(15) (2009) 2273-82.

[31] L. Fornelli, J. Parra, R. Hartmer, C. Stoermer, M. Lubeck, Y.O. Tsybin, Top-down analysis of 30-80 kDa proteins by electron transfer dissociation time-of-flight mass spectrometry, Anal Bioanal Chem (2013).

[32] Z. Tian, N. Tolic, R. Zhao, R.J. Moore, S.M. Hengel, E.W. Robinson, D.L. Stenoien, S. Wu, R.D. Smith, L. Pasa-Tolic, Enhanced top-down characterization of histone post-translational modifications, Genome Biol 13(10) (2012) R86.

[33] D.R. Ahlf, P.D. Compton, J.C. Tran, B.P. Early, P.M. Thomas, N.L. Kelleher, Evaluation of the compact high-field orbitrap for top-down proteomics of human cells, J Proteome Res 11(8) (2012) 4308-14.

[34] Y.O. Tsybin, L. Fornelli, C. Stoermer, M. Luebeck, J. Parra, S. Nallet, F.M. Wurm, R. Hartmer, Structural Analysis of Intact Monoclonal Antibodies by Electron Transfer Dissociation Mass Spectrometry, Analytical Chemistry 83(23) (2011) 8919-8927.

[35] A. Michalski, E. Damoc, O. Lange, E. Denisov, D. Nolting, M. Muller, R. Viner, J. Schwartz, P. Remes, M. Belford, J.J. Dunyach, J. Cox, S. Horning, M. Mann, A. Makarov, Ultra high resolution linear ion trap Orbitrap mass spectrometer (Orbitrap Elite) facilitates top down LC MS/MS and versatile peptide fragmentation modes, Mol Cell Proteomics 11(3) (2012) O111 013698.

[36] A. Makarov, E. Denisov, O. Lange, Performance evaluation of a high-field Orbitrap mass analyzer, J Am Soc Mass Spectrom 20(8) (2009) 1391-6.

[37] Y.O. Tsybin, Structural Analysis of Complex Molecular Systems by High-Resolution and Tandem Mass Spectrometry, in: B. Pignataro (Ed.), Discovering the Future of Molecular Sciences, Wiley-VCH Verlag GmbH & Co. KGaA2014.

[38] O. Lange, E. Damoc, A. Wieghaus, A. Makarov, Enhanced Fourier transform for Orbitrap mass spectrometry, International Journal of Mass Spectrometry 369 (2014) 16-22.

[39] E. Denisov, E. Damoc, O. Lange, A. Makarov, Orbitrap mass spectrometry with resolving powers above 1,000,000, International Journal of Mass Spectrometry 325 (2012) 80-85.

[40] J.V. Olsen, B. Macek, O. Lange, A. Makarov, S. Horning, M. Mann, Higher-energy C-trap dissociation for peptide modification analysis, Nat Methods 4(9) (2007) 709-12.

[41] C.K. Frese, A.F. Altelaar, H. van den Toorn, D. Nolting, J. Griep-Raming, A.J. Heck, S. Mohammed, Toward full peptide sequence coverage by dual fragmentation combining electron-transfer and higher-energy collision dissociation tandem mass spectrometry, Anal Chem 84(22) (2012) 9668-73.

[42] A.M. Brunner, P. Lossl, F. Liu, R. Huguet, C. Mullen, M. Yamashita, V. Zabrouskov, A. Makarov, A.F. Altelaar, A.J. Heck, Benchmarking multiple fragmentation methods on an orbitrap fusion for top-down phospho-proteoform characterization, Anal Chem 87(8) (2015) 4152-8.

[43] Y. Zheng, L. Fornelli, P.D. Compton, S. Sharma, J. Canterbury, C. Mullen, V. Zabrouskov, R.T. Fellers, P.M. Thomas, J.D. Licht, M.W. Senko, N.L. Kelleher, Unabridged Analysis of Human Histone H3 by Differential Top-Down Mass Spectrometry Reveals Hypermethylated Proteoforms from MMSET/NSD2 Overexpression, Mol Cell Proteomics 15(3) (2016) 776-90.

[44] S. Rosati, R.J. Rose, N.J. Thompson, E. van Duijn, E. Damoc, E. Denisov, A. Makarov, A.J. Heck, Exploring an orbitrap analyzer for the characterization of intact antibodies by native mass spectrometry, Angew Chem Int Ed Engl 51(52) (2012) 12992-6.

[45] M.W. Senko, J.D. Canterbury, S. Guan, A.G. Marshall, A high-performance modular data system for Fourier transform ion cyclotron resonance mass spectrometry, Rapid Commun Mass Spectrom 10(14) (1996) 1839-44.

[46] X. Liu, Y. Inbar, P.C. Dorrestein, C. Wynne, N. Edwards, P. Souda, J.P. Whitelegge, V. Bafna, P.A. Pevzner, Deconvolution and database search of

complex tandem mass spectra of intact proteins: a combinatorial approach, Mol Cell Proteomics 9(12) (2010) 2772-82.

[47] R.T. Fellers, J.B. Greer, B.P. Early, X. Yu, R.D. LeDuc, N.L. Kelleher, P.M. Thomas, ProSight Lite: graphical software to analyze top-down mass spectrometry data, Proteomics 15(7) (2015) 1235-8.

[48] K. Breuker, H. Oh, C. Lin, B.K. Carpenter, F.W. McLafferty, Nonergodic and conformational control of the electron capture dissociation of protein cations, Proc Natl Acad Sci U S A 101(39) (2004) 14011-6.

[49] C.M. Rose, J.D. Russell, A.R. Ledvina, G.C. McAlister, M.S. Westphall, J. Griep-Raming, J.C. Schwartz, J.J. Coon, J.E. Syka, Multipurpose dissociation cell for enhanced ETD of intact protein species, J Am Soc Mass Spectrom 24(6) (2013) 816-27.

[50] L. Earley, L.C. Anderson, D.L. Bai, C. Mullen, J.E. Syka, A.M. English, J.J. Dunyach, G.C. Stafford, Jr., J. Shabanowitz, D.F. Hunt, P.D. Compton, Front-end electron transfer dissociation: a new ionization source, Anal Chem 85(17) (2013) 8385-90.

[51] J.B. Shaw, W.Z. Li, D.D. Holden, Y. Zhang, J. Griep-Raming, R.T. Fellers, B.P. Early, P.M. Thomas, N.L. Kelleher, J.S. Brodbelt, Complete Protein Characterization Using Top-Down Mass Spectrometry and Ultraviolet Photodissociation, Journal of the American Chemical Society 135(34) (2013) 12646-12651.

Figure captions

Figure 1. Top-down ETD Orbitrap FTMS of IgG1 (adalimumab) with ion-ion interaction time of 10 and 25 ms. (A) Combined mass spectrum including transients from both 10 and 25 ms measurements, with product ion population arising from the former experiment highlighted in blue, and from the latter indicated in red. (B) and (C) Expanded views of the two product ion populations, with assigned product ions derived from the heavy chain. Note the difference in the average charge state of the product ions of the two populations.

Figure 2. Fragmentation map of adalimumab by top-down Orbitrap FTMS. (A) ETD MS/MS. (B) EThcD MS/MS. The heavy chain information is on top, the light chain information is at the bottom.

Figure 3. Product ion abundance analysis of ETD top-down MS of adalimumab with 10 ms ETD duration and trastuzumab with 10 and 25 ms duration. In the case of trastuzumab, the color-coded histogram demonstrates the improvement in sequence coverage obtained through the combination of 10 ms (magenta) and 25 ms (cyan) ETD MS/MS data. Whereas medium and large product ions (e.g., z_{117} and z_{63}) are generally produced using 10 ms duration, smaller ions such as z_{16}, z_{17} and z_{18} are detected only in the case of a longer ETD duration, presumably as the result of secondary fragmentation (i.e., re-fragmentation of larger product ions).

Figure 4. Color-coded representation of ETD PIA results for the C-terminus of the heavy chain of trastuzumab. (A) 10 ms ETD. (B) 25 ms ETD. The displayed image is based on X-ray crystallography data (PDB entry: 3D6G).

Figure 5. Fragmentation map of panitumumab (IgG2) obtained with top-down ETD Orbitrap FTMS.

Table 1. Sequence coverage obtained for different IgGs1 and IgG2 by top-down ETD Orbitrap FTMS. Indicated scans consist of 10 microscans each. Note, only *c*- and *z*-type ions were considered for ETD MS (for both "high-field" and "standard" Orbitrap data), whereas also *b*- and *y*-type ions were included in EThcD MS analysis.

Table 1.

		Light chain				*Heavy chain*				Total sequence coverage
	Number of scans	N-terminal product ions	C-terminal product ions	Unique cleavage sites	Sequence coverage	N-terminal product ions	C-terminal product ions	Unique cleavage sites	Sequence coverage	
high-field Orbitrap										
Adalimumab ETD	310	34	19	41	19.2%	39	78	117	26.0%	23.8%
Adalimumab EThcD	260	45	29	59	27.7%	22	58	80	17.8%	21.0%
Adalimumab combined	570	50	32	67	31.5%	53	82	135	30.0%	30.5%
Trastuzumab ETD	310	37	19	45	21.1%	55	75	130	29.0%	26.5%
Panitumumab ETD	300	34	9	34	15.9%	23	83	106	23.9%	21.3%
standard Orbitrap										
Adalimumab combined	1360	54	59	84	39.4%	60	79	119	26.4%	30.6%

Figure 1.

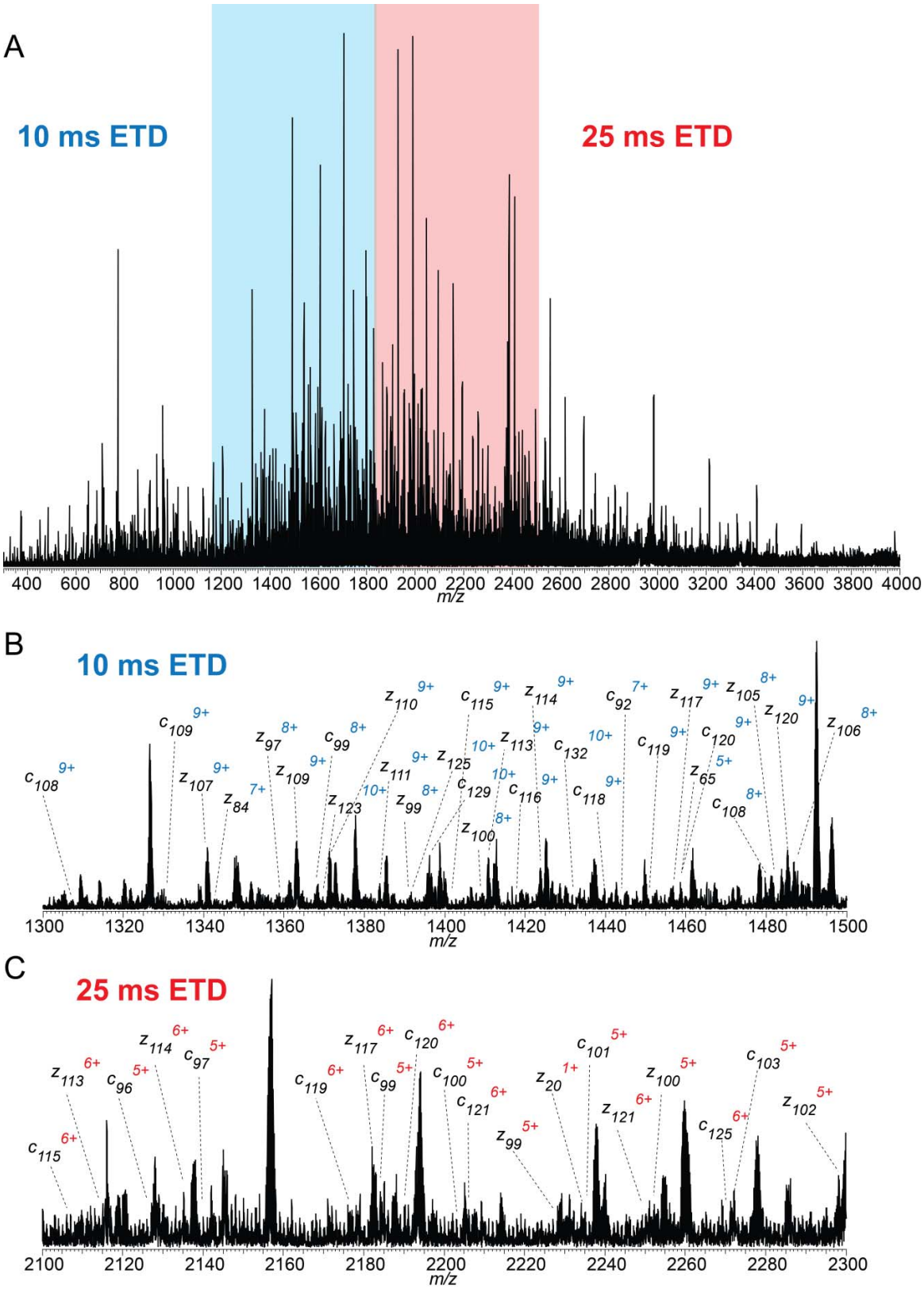
A
10 ms ETD
25 ms ETD
400 600 800 1000 1200 1400 1600 1800 2000 2200 2400 2600 2800 3000 3200 3400 3600 3800 4000
m/z
B
10 ms ETD
1300 1320 1340 1360 1380 1400 1420 1440 1460 1480 1500
m/z
C
25 ms ETD
2100 2120 2140 2160 2180 2200 2220 2240 2260 2280 2300
m/z

Figure 2.

Figure 3.

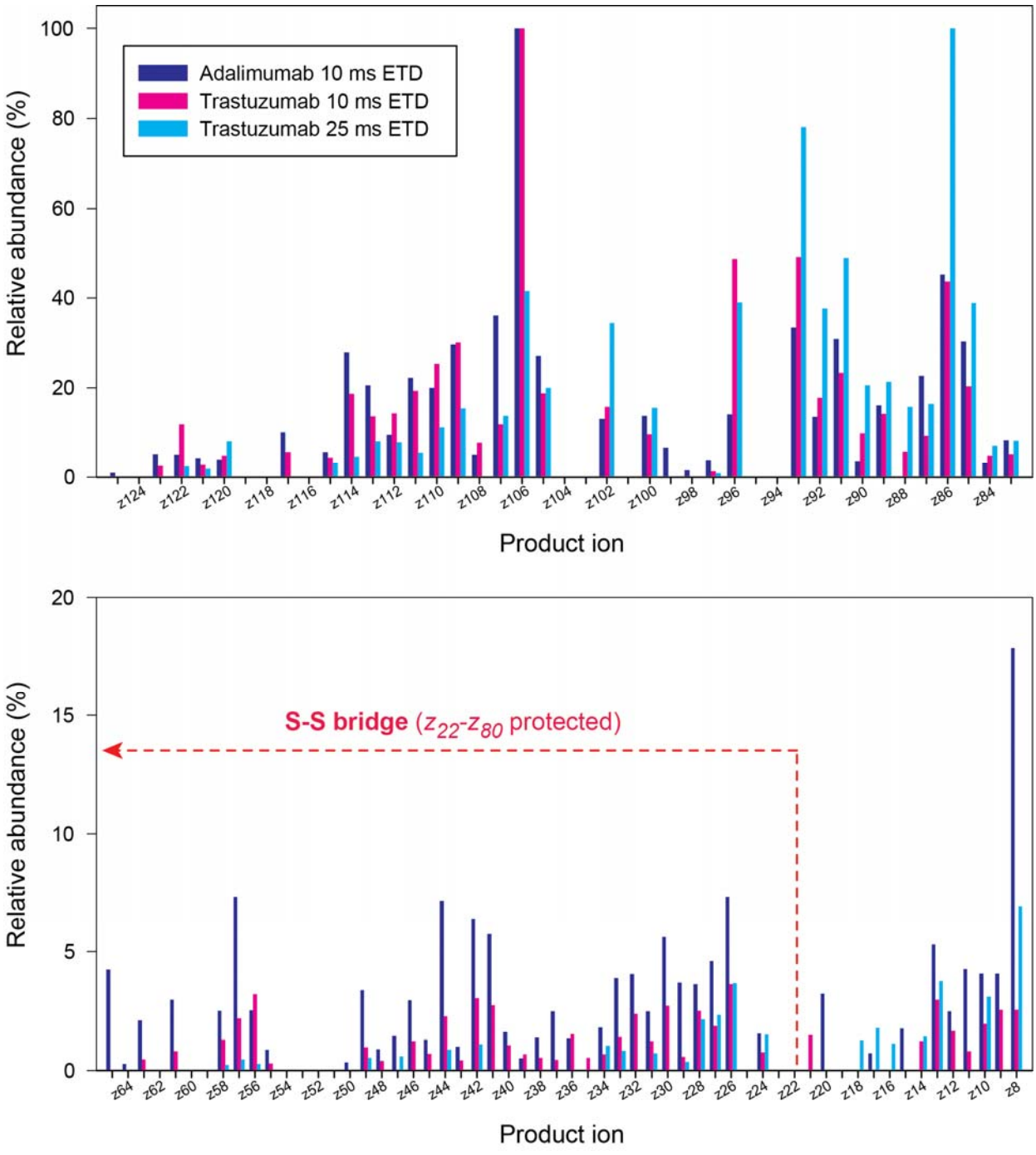
Adalimumab 10 ms ETD
Trastuzumab 10 ms ETD
Trastuzumab 25 ms ETD
Relative abundance (%)
Product ion
S-S bridge (z_{22}-z_{80} protected)
Relative abundance (%)
Product ion

Figure 4.

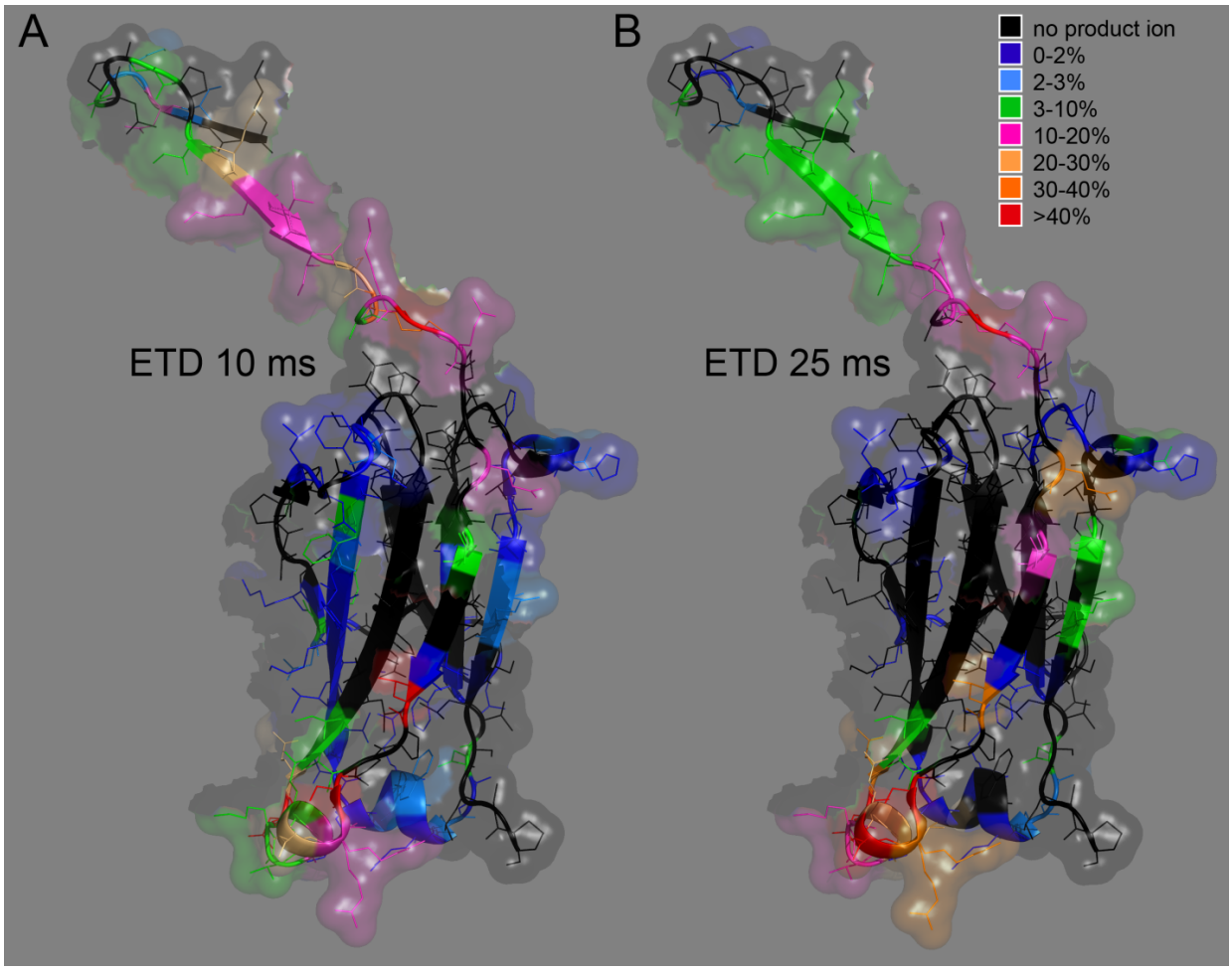

Figure 5.


Q V Q L Q E S G P G L V K P S E T L S L T C T V S
G G S V S S G D Y Y W T W I R Q S P G K G L E W I
G H I Y Y S G N T N Y N P S L K S R L T I S I D T
S K T Q F S L K L S S V T A A D T A I Y Y C V R D
R V T G A F D I W G Q G T M V T V S S A S T K G P
S V F P L A P C S R S T S E S T A A L G C L V K D
Y F P E P V T V S W N S G A L T S G V H T F P A V
L Q S S G L Y S L S S V V T V P S S N F G T Q T Y
T C N V D H K P S N T K V D K T V E R K C C V E C
P P C P A P P V A G P S V F L F P P K P K D T L M
I S R T P E V T C V V V D V S H E D P E V Q F N W
Y V D G V E V H N A K T K P R E E Q F N S T F R V
V S V L T V V H Q D W L N G K E Y K C K V S N K G
L P A P I E K T I S K T K G Q P R E P Q V Y T L P
P S R E E M T K N Q V S L T C L V K G F Y P S D I
A V E W E S N G Q P E N N Y K T T P P M L D S D G
S F F L Y S K L T V D K S R W Q Q G N V F S C S V
M H E A L H N H Y T Q K S L S L S P G K

D I Q M T Q S P S S L S A S V G D R V T I T C Q A
S Q D I S N Y L N W Y Q Q K P G K A P K L L I Y D
A S N L E T G V P S R F S G S G S G T D F T F T I
S S L Q P E D I A T Y F C Q H F D H L P L A F G G
G T K V E I K R T V A A P S V F I F P P S D E Q L
K S G T A S V V C L L N N F Y P R E A K V Q W K V
D N A L Q S G N S Q E S V T E Q D S K D S T Y S L
S S T L T L S K A D Y E K H K V Y A C E V T H Q G
L S S P V T K S F N R G E C